Knockdown of SIPA1L3 Inhibits the Proliferation and Invasion of Non–Small Cell Lung Cancer Cells Through the Hippo Pathway

Si Wang
China Medical University
Qiang Han
China Medical University
Xue-Zhu Rong
China Medical University
Ming-Fang Sun
China Medical University
Ke-Xin Diao
China Medical University
En-Hua Wang
China Medical University College of Medicine
Yang Liu (liuyanglovebee@163.com)
China Medical University College of Medicine

Research

Keywords: non-small cell lung cancer, SIPA1L3, Hippo signaling pathway, AMOT

Posted Date: February 26th, 2021

DOI: https://doi.org/10.21203/rs.3.rs-243266/v1

Abstract

Background: SIPA1L3 is a member of the signal-induced proliferation-associated (SIPA) protein family, only limited data about the SIPA1L3 are currently available in human carcinoma. Our present study provides the expression pattern and function of SIPA1L3 in non-small cell lung cancer (NSCLC).

Methods: We performed immunohistochemistry to detect the distribution of SIPA1L3 in NSCLC specimens and analyzed the relationship between SIPA1L3 expression and patients clinicopathological feature. We used small interfering RNA (siRNA) to specifically silence SIPA1L3, then investigated its effect on cell growth and invasion in human lung cancer cell lines. Western blot and immunoprecipitation were performed to show the interaction of SIPA1L3 with the core proteins of Hippo pathway, and the Hippo pathway activity.

Results: Immunohistochemical staining showed that SIPA1L3 was cytoplasmic increasing in 147 of 217 cases. High levels of SIPA1L3 expression were associated with poor differentiation and a high tumor node metastasis stage, positive lymph nodal status, and poor prognosis. Downregulation of SIPA1L3 inhibited cell EMT, growth, and invasion. As well as SIPA1L3 inhibited Hippo pathway. SIPA1L3 interacted with AMOT, which inhibited AMOT binding to Pals, then decreased nuclear location of YAP.

Conclusions: SIPA1L3 overexpression may be a marker for advanced NSCLC. SIPA1L3 reduction inhibits the proliferative and invasive ability of the lung cancer cells, which involves the Hippo pathway by contacting with AMOT.

1. Introduction

Of all the malignant tumors, lung cancer currently has the highest incidence and mortality, with 85% to 90% of these cancers being non–small cell lung cancer (NSCLC) [1-3]. A variety of factors critical for cell adhesion, cell polarity and cellular structure are mutated in human lung cancer, however not all are currently known.

SIPA1L3 is a member of the signal-induced proliferation-associated (SIPA) protein family, which was also known as the part of the Rap GTPase activating protein (RapGAPs) superfamily. The SIPA protein family comprises four members, SIPA1, SIPA1L1, SIPA1L2, and SIPA1L3[4-6]. All SIPA proteins are expressed in the central nervous system, and basically most of the studies focused on their function within the brain. Beside it, SIPA1L3 expression has been described in the embryonic lens and mutations of the human SIPA1L3 gene result in congenital cataracts [7-9]. These results showed that SIPA1L3 has an important role in epithelial cell morphogenesis, establishing or maintaining cell polarity, cell adhesion, and cytoskeletal organization. They also indicated that SIPA1L3 is a novel molecular factor contributing to epithelial cellular function, and SIPA1L3 is a causative disease gene. However, the functional role of Sipa1l3 in human carcinoma, including NSCLC, remain largely unclear.

All SIPA family members share common domains, namely an N-terminal Rap GAP domain (Rap-GTPase activating domain), a PDZ domain and a C-terminal coiled-coil domain carrying a leucin-zipper motif. SIPA1L1-SIPA1L3 contains an additional domain of unknown function (DUF3401) [6-8]. Base on its functional structure, we hypothesized that SIPA1L3 play an important functional role in lung cancer development. In this study, we investigated whether SIPA1L3 has the abnormal expression in NSCLCs, and its influence on cell proliferation and invasion. As well as the underlying molecular pathways involving in the progression of NSCLC.

2. Materials And Methods

2.1 Specimen Collection

217 specimens were randomly obtained either by biopsy or complete resection from patients with NSCLC at the First Affiliated Hospital of China Medical University. According to the 2015 World Health Organization (WHO) lung cancer histopathological diagnostic criteria, 123 cases were adenocarcinoma and 94 were squamous cell carcinoma (SCC). According to the eighty edition of the American Joint Committee on Cancer TNM staging criteria published by the International Association for the Study of Lung Cancer in 2017, 135 cases were stage I-II and 82 cases were stage III-IV. None of them was treated with radiotherapy, chemotherapy, or TKIs before definitive pathological diagnoses were determined.

The present study was conducted with the approval of the China Medical University Local Institutional Review Board (2017025). Informed consent was obtained from all the patients for analysis of their specimens.

2.2 Immunohistochemistry Staining

Immunohistochemistry assays were performed as described previously [10]. Briefly, tissue sections were incubated with normal goat serum to block nonspecific antibody binding and then with mouse monoclonal anti-SIPA1L3. (1:100; Cell Signaling Technology (CST) Inc., Danvers, Massachusetts). Positive SIPA1L3 expression was determined by the intensity of cytoplasm staining of tumor cells and the proportion of SIPA1L3-positive cells in the tissue sections. The immunostaining assessment scale as follows: negative (no staining), weak (light yellow staining, no clear granular or yellow staining, and clear granular staining area <10%), moderate (yellow staining and clear granular staining area ≥10% or brown staining and clear granular staining area <10%), or strong (brown staining and clear granular staining area ≥10%). Negative to weak were considered to be normal SIPA1L3 expression and moderate to strong were considered to be SIPA1L3 overexpression. Two investigators blinded to the clinical data independently and randomly examined all tumor slides.

2.3. Western blot analysis

Western blot assays were performed as described previously [11]. Protein concentration was determined with a bicinchoninic acid (BCA) kit (Pierce, Rockford, IL, USA). Equal amounts of lysate were separated by

SDS-PAGE and western blot. The primary antibodies against YAP (#14074, 1:500), MST1 (#14946, 1:500), phospho-MST1 (#49332, 1:500), LATS1 (#3477, 1:500), phospho-LATS1 (#9157, 1:500), GAPDH (#5174, 1:10000), and AMOT (#43130, 1:500) were purchased from CST Inc (Danvers, MA, USA). Primary antibodies against LaminB1 (#ab16048, 1:1000/IB) were purchased from Abcam. Cyclin E (sc-377100, 1:200), Pals (sc-365411, 1:200), E-cadherin (sc-8426, 1:200), N-cadherin (sc-8424, 1:200), ZO-1(sc-33725, 1:200), Vimentin (sc-6260, 1:200), Snail (sc-166476, 1:200), a-SMA (sc-53142, 1:200), and CTGF (sc-34772, 1:200) were from Santa Cruz Biotechnology (Santa Cruz, California). SIPA1L3 (HPA045480, 1:500) was from Sigma (Merck Life Science (Shanghai) Co., Ltd. Shanghai, China). Secondary antibodies were purchased from CST Inc. Expression was quantified using densitometry and ImageJ software, the protein bands were visualized with ECL western blotting substrate (Pierce, Rockford, IL, USA) and the BioImaging System (UVP Inc.,Upland, CA, USA), which were normalized to GAPDH.

2.4. Cell lines and transfection

The human bronchial epithelial cells (HBEs), a human adenocarcinoma cell line (A549, LTEP-a-2, H1299), and an SCC cell line (LK-2, SK-MES-1) were purchased from ATCC (Manassas, VA, USA). The SIPA1L3-siRNA and the negative controls were purchased from Genechem Biological Technology Co. Ltd. (Shanghai, China). The cells were transfected with plasmids using Attractene transfection reagent (Qiagen, Hilden, Germany) according to the manufacturer's instructions.

2.5. 3-(4,5-dimethylthiazol-2-yl)-2,5-diphenyltetrazolium bromide (MTT) assay

Cells were inoculated into 96-well plates and 5 mg mL-l MTT (Sigma-Aldrich Corp., St. Louis, MO, USA) was added to each well. Then 200 μL dimethyl sulfoxide (DMSO) was added to each well and the plates were shaken for 10 min to dissolve the formazan crystals. OD490 was measured in amicroplate reader (Model 550; Bio-Rad Laboratories, Hercules, CA, USA).

2.6. Matrigel Invasion Assay

The cell invasion assay was performed in a 24-well Transwell chamber with an 8-μm pore size (Costar, Cambridge, MA). Inserts were coated with 20 μL Matrigel (1:3 dilution; BD Bioscience). Forty-eight hours after transfection, 3×10^5 cells in 100 μL of serum-free medium were transferred to the upper Matrigel chamber and incubated for 16 hours, whereas 600 μL of culture medium supplemented with 10% fetal bovine serum was placed in the lower chamber. After 18 hours of incubation, the noninvaded cells were removed from the upper membrane surface with a cotton swab, and the cells that passed through the filter were fixed with 4% paraformaldehyde and stained with hematoxylin. The number of invaded cells was counted in 10 randomly selected high-power fields under a microscope. This experiment was performed in triplicates.

2.7. Colony Formation Assay

Cells were plated into 6-cm cell culture dishes (1000 cells per dish) and incubated for 14 days. The plates were washed with phosphate buffered saline, fixed with 4% paraformaldehyde, and stained with Giemsa. Colonies containing >50 cells were counted under a microscope. Images were made and the number of colonies was established manually.

2.8. Statistical analysis

SPSS v. 22.0 (IBM Corp., Armonk, NY, USA) was used for all analyses. Each cell line experiment was performed in triplicate. The western blot gray value was detected with Image Lab^{TM} (Bio-Rad Laboratories, Hercules, CA, USA) and compared by Student's t-test. $P< 0.05$ indicated statistical significance.

3. Results

3.1. Overexpression of SIPA1L3 correlated with malignant phenotype in NSCLC patients

The database from TCGA indicated that lung cancer patients with increased SIPA1L3 showed higher mRNA level (Supplementary Fig.1) and poorer overall survival (Supplementary Fig. 2). We performed immunohistochemical analysis of 217 NSCLC tissues to testify them. SIPA1L3 was undetectable (−) or weak positive in normal bronchial epithelia or pneumocytes. In 147 of 217 (67.74%) lung cancer specimens, SIPA1L3 showed increased cytoplasmic expression (Fig. 1). To identify the clinical significance of SIPA1L3 in NSCLC tissues, we analyzed the correlation between SIPA1L3 overexpression and clinicopathologic parameters. As summarized in Table 1, tumors with increased SIPA1L3 tended to display more malignant phenotypes, such as the lower differentiation ($P = 0.016$), the greater clinical tumor size ($P = 0.003$), the higher tumor node metastasis (TNM) stage ($P = 0.010$), and positive lymphatic metastasis ($P = 0.004$). In terms of survival, patients with SIPA1L3 overexpression had a poorer overall survival than patients with normal SIPA1L3 expression ($P < 0.001$; Fig. 2). Western blot analysis was performed in lung cancer tissues and cell lines, which were consistent with the IHC results (Fig. 3). These results suggest that SIPA1L3 acts as a tumor promoter in NSCLC.

3.2. Downregulation of SIPA1L3 by siRNA in lung cancer cells inhibited lung cancer cell growth and invasion

After transfection with SIPA1L3-siRNAs in LTEP-a-2 and LK-2 cell lines, decreased SIPA1L3 inhibited the proliferation of LTEP-a-2 and LK-2 cells (Fig. 4A). As shown in Fig. 4B, SIPA1L3 silencing resulted in a significant increase in G1-phase cells and a significant reduction in S-phase cells. In addition, in the cells with SIPA1L3 knockdown, a significant increase was observed in the population of cells undergoing early and late apoptosis (Fig. 4C). As well as SIPA1L3 significantly reduced colony numbers and the size of the lung cancer cells (Fig. 4D). These data indicated that SIPA1L3 has the effect on the regulation of the cell cycle and apoptosis, thus regulated the cell growth of lung cancer cells. Furthermore, we observed that decreased expression of SIPA1L3 reduced the cell invasion significantly, comparing with the controls (Fig. 4E).

3.3. SIPA1L3 knockdown inhibited epithelial to mesenchymal transition.

The cell-biological program termed the epithelial-to-mesenchymal transition (EMT) plays an important role in the process of malignant progression [12-14]. In the LTEP-a-2 and LK-2 cell lines with SIPA1L3-siRNA, the expression of E-cadherin and ZO-1 was significantly up-regulated, while the expression of N-cadherin, vimentin, snail and a-SMA was significantly down-regulated. EMT is inhibited in the SIPA1L3-deleption lung cancer cells. Thus, SIPA1L3 may contribute to the carcinoma processes by inducing EMT.

3.4. SIPA1L3 depletion is accompanied with Hippo signal pathway activation.

The Hippo signaling pathway was first discovered and studied in Drosophila melanogaster, and it has been demonstrated to play crucial roles in lung cancer [15-17]. We are using immunoblotting to detect the difference in the expression of Hippo pathway-related proteins between the lung cancer cells and the cells with SIPA1L3-siRNA. The expression of p-MST1 and p-LATS1 was upregulated, whereas Cyclin E, CTGF, and the nuclear YAP was downregulated, compared to those in control LTEP-a-2 and LK-2 cells. These results indicated that advanced carcinoma by SIPA1L3 may be closely related to the inhibition of the Hippo pathway.

3.5. Combination of SIPA1L3 and AMOT Inhibits the Hippo Pathway

AMOTs is involved in Hippo signaling pathway through interacting with multiple core proteins on this pathway. It formed AMOT-mediated complex, such as AMOT-Pals-Merlin-Patj complex, activating Hippo pathway. In the C-terminal region of AMOT, it composes of the PDZ-binding domain [18-20]. Base on SIPA1L3 possessing PDZ domain, we used SIPA1L3 and AMOT antibody for immunoprecipitation, respectively, and the obtained proteins were detected by western blot. We found that SIPA1L3 and AMOT interacted with each other. Furthermore, AMOT binding to Pals increased after interfering with SIPA1L3, and nuclear YAP decreased. In the cell lines with SIPA1L3-cDNA, immunoprecipitation revealed that the binding of AMOT to SIPA1L3 increased but the binding of AMOT to Pals decreased. YAP is upregulated and translocated into the nucleus.

4. Discussion

Recently, the SIPA1L3 has also been associated with congenital human cataracts [6-8]. As expression data of the SIPA1L3 during the embryogenesis and disease, it provides a good basis for further functional studies. Here, we present the expression and significance analysis of SIPA1L3 in lung cancer.

Firstly, we examined the subcellular localization of endogenous SIPA1L3 in lung tissues by immunohistochemical staining. The SIPA1L3 protein was weakly detectable or undetectable in normal bronchial epithelium, and 67.74% of examined NSCLC tissues showed elevated cytoplasm expression. Clinically, a direct correlation was observed between upregulated SIPA1L3 and an advanced tumor stage, lymph nodal status, and poor differentiation. This implies the tumor-promoting function of SIPA1L3 as a cytoplasmic protein in NSCLC.

Following the evaluation of SIPA1L3 expression patterns in NSCLC, we explored the role of activated SIPA1L3 in regulating NSCLC cell proliferation and invasion. Knockdown of SIPA1L3 in LTEP-a-2 and LK-2 cells, resulted in a significant decrease in the cell proliferation and the invasion capacity of the lung cancer cells.

The Sipa1l3-/- mutant mice showed a failure in the maintenance of epithelial cell properties in the lens. Failure in the maintenance of epithelial cell properties can result in abnormal EMT, which is characterized by the disassembly of cell adhesion, loss of polarity and the acquisition of migratory capacity [8]. We further testified that SIPA1L3 prompted EMT program. The increased motility/invasiveness associated with the mesenchymal cell state has linked the EMT program with metastasis, in which cell separation from the primary tumor mass can be considered as the first step of the invasion-metastasis cascade. Thus, a variety of studies have demonstrated that induction of an EMT program allows carcinoma cells to lose cell-cell junctions, degrade local basement membrane via elevated expression of various matrix-degrading enzymes, and thus support their migration and invasion [21-24]. Therefore, SIPA1L3 overexpression promotes malignant lung cell growth, invasion, and EMT, which may explain our findings that SIPA1L3 overexpression was the major defining characteristic of NSCLC tumors and correlated with several clinicopathological factors.

We further investigated possible mechanisms underlying the role of SIPA1L3 in cell proliferation and invasion next. The Hippo pathway controls cell proliferation, differentiation, invasion, and survival by regulating the main downstream effector molecules Yes-associated protein (YAP). The major YAP regulators are the kinases LATS1/2 and MST1/2, which phosphorylate and inhibit YAP [25-27]. After interference with SIPA1L3, we found that p-MST1 and p-LATS1 was upregulated, while the nuclear YAP was decreased. So, SIPA1L3 inhibited the Hippo signal pathway in lung cancer.

An AMOT-dependent complex, which comprised of AMOT, Pals, Merlin, and Patj, functions upstream of the core Hippo pathway kinases LATS1/2 and MST1/2 [18, 19]. Based on the predicted domain structure of SIPA1L3, it possesses an N-terminal PDZ domains, which is predicted to be required for protein-protein interactions. While AMOT has the C-terminal PDZ-binding motifs, we use immunocoprecipitation to identify the interaction between SIPA1L3 and AMOT. In accordance with previous findings, immunocoprecipitation also indicated an interaction between AMOT and Pals. Furthermore, we found that SIPA1L3 inhibited the binding of AMOT to Pals and the phosphorylation of YAP, then increased the nuclear location of YAP. It has been shown that the PDZ-binding motifs of the Amot binds Pals, thus SIPA1L3 and Pals could competitively bind with AMOT PDZ-binding motifs. Knockdown of SIPA1L3 decreased its combination with AMOT, then enhanced the combination of AMOT PDZ-binding motifs with Pals, which prompted the AMOT-dependent complex (AMOT, Pals, Merlin, and Patj). The phosphorylate kinases LATS1/2 and MST1/2 were increased, then inactives YAP through phosphorylation, resulting in YAP degradation. Reduced YAP nuclear localization ultimately prevents the proliferation and invasion of lung cancer cells.

5. Conclusion

Clinical tumor analysis in this study strongly supports that SIPA1L3 is a tumor oncogene in NSCLC. Our results from cellular experiments demonstrate that SIPA1L3 reduction inhibits cells' proliferative and invasive ability, which involves the Hippo pathway. Although AMOT-medicated complex is one manner of the regulation Hippo pathway by SIPA1L3, but AMOT play multiple functions in its influence on Hippo signaling. Further studies will be required to determine the other manners of SIPA1L3 regulating the Hippo pathway, which mediated by AMOT. Taken together, although there is a limited understanding of SIPA1L3's role in cancer tumorigenesis, we identified SIPA1L3 as a novel candidate gene. It paves the way for improvements in our understanding of lung cancer malignant phenotype development.

6. List Of Abbreviations

signal-induced proliferation-associated (SIPA); non-small cell lung cancer (NSCLC); interfering RNA (siRNA); Rap GTPase activating protein (RapGAPs); World Health Organization (WHO); squamous cell carcinoma (SCC); bicinchoninic acid (BCA); human bronchial epithelial cells (HBEs); tumor node metastasis (TNM); epithelial-to-mesenchymal transition (EMT); Yes-associated protein (YAP).

7. Declarations

Ethics approval and consent to participate

The present study was conducted with the approval of the China Medical University Local Institutional Review Board (2017025). Informed consent was obtained from all the patients for analysis of their specimens.

Consent for publication

Not applicable.

Availability of data and material

Not applicable.

Competing interests

Not applicable.

Funding

This study was funded by the Natural Science Foundation of Liao Ning Province of China (grant number 20180530045).

Authors' contributions

SW wrote the paper; SW, QH, XZR, and MFS performed the research; EHW and YL designed the research study; SW and KXD analyzed the data.

Acknowledgement

We would like to thank Editage for English language editing.

References

1. Heydt C, Michels S, Thress KS, Bergner S, Wolf J, Buettner R. Novel approaches against epidermal growth factor receptor tyrosine kinase inhibitor resistance. Oncotarget 2018;9:15418-15434. https://doi: 10.18632/oncotarget.24624.
2. Novello S, Barlesi F, Califano R, et al. Metastatic non–small-cell lung cancer: ESMO clinical practice guidelines for diagnosis, treatment and follow-up. Ann Oncol 2016;27:v1-v27. https://doi: 10.1093/annonc/mdw326.
3. Ribaudo G, Zanforlin E, Zagotto G. Overcoming resistance in non–small-lung cancer: a practical lesson for the medicinal chemist. Arch Pharm (Weinheim) 2018;351:e1800037. https://doi: 10.1002/ardp.201800037.
4. Evers C, Paramasivam N, Hinderhofer K, et al. SIPA1L3 identified by linkage analysis and whole-exome sequencing as a novel gene for autosomal recessive congenital cataract. Eur J Hum Genet 2015;23:1627-1633. https://doi: 10.1038/ejhg.2015.46.
5. Dolnik A, Kanwal N, Mackert S, et al. Sipa1l3/SPAR3 is targeted to postsynaptic specializations and interacts with the Fezzin ProSAPiP1/Lzts3. J Neurochem 2016;136:28-35. https://doi: 10.1111/jnc.13353.
6. Rothe M, Monteiro F, Dietmann P, Kühl SJ. Comparative expression study of sipa family members during early Xenopus laevis development. Dev Genes Evol 2016;226:369-382. https://doi: 10.1007/s00427-016-0556-1.
7. Rothe M, Kanwal N, Dietmann P, et al. An Epha4/Sipa1l3/Wnt pathway regulates eye development and lens maturation. Development 2017;144:321-333. https://doi: 10.1242/dev.147462.
8. Greenlees R, Mihelec M, Yousoof S, et al. Mutations in SIPA1L3 cause eye defects through disruption of cell polarity and cytoskeleton organization. Hum Mol Genet 2015;24:5789-5804. https://doi: 10.1093/hmg/ddv298.
9. Wang L, Li P, Guo X. Screening of methylation genes in age-related cataract. Int J Ophthalmol 2018;11:1102-1107. https://doi: 10.18240/ijo.2018.07.05.
10. Liu Y, Dong QZ, Wang S, et al. Abnormal expression of Pygopus 2 correlates with a malignant phenotype in human lung cancer. BMC Cancer 2013;13:346.
11. Wang S, Wang SY, Du F, et al. Knockdown of PAK1 Inhibits the Proliferation and Invasion of Non-Small Cell Lung Cancer Cells Through the ERK Pathway. Appl Immunohistochem Mol Morphol 2020;28:602-610. https://doi: 10.1186/1471-2407-13-346.

12. Zhang Y, Weinberg RA. Epithelial-to-mesenchymal transition in cancer: complexity and opportunities. Front Med 2018;12:361-373. https://doi: 10.1007/s11684-018-0656-6.
13. Lamouille S, Xu J, Derynck R. Molecular mechanisms of epithelial-mesenchymal transition. Nat Rev Mol Cell Biol 2014;15:178-196. https://doi: 10.1038/nrm3758.
14. Dongre A, Weinberg RA. New insights into the mechanisms of epithelial-mesenchymal transition and implications for cancer. Nat Rev Mol Cell Biol 2019;20:69-84. https://doi: 10.1038/s41580-018-0080-4.
15. Harvey KF, Zhang X, Thomas DM. The Hippo pathway and human cancer. Nat Rev Cancer 2013;13:246-257. https://doi: 10.1038/nrc3458.
16. Poma AM, Torregrossa L, Bruno R, Basolo F, Fontanini G. Hippo pathway affects survival of cancer patients: extensive analysis of TCGA data and review of literature. Sci Rep 2018;8:10623. https://doi: 10.1038/s41598-018-28928-3.
17. Fu SL, Zhao WY, Zhang WJ, Song H, Ji HB, Tang N. Hippo signaling pathway in lung development, regeneration, and diseases. Yi Chuan 2017;39:597-606. https://doi: 10.16288/j.yczz.17-056.
18. Chang YC, Wu JW, Wang CW, Jang AC. Hippo signaling-mediated mechanotransduction in cell movement and cancer metastasis. Front Mol Biosci 2020;6:157. https://doi: 10.3389/fmolb.2019.00157.
19. Huang T, Zhou Y, Zhang J, et al. The physiological role of Motin family and its dysregulation in tumorigenesis. J Transl Med 2018;16:98. https://doi: 10.1186/s12967-018-1466-y.
20. Levchenko T, Bratt A, Arbiser JL, Holmgren L. Angiomotin expression promotes hemangioendothelioma invasion. Oncogene 2004;23:1469-1473. https://doi: 10.1038/sj.onc.1207264.
21. Walter C, Davis JT, Mathur J, Pathak A. Physical defects in basement membrane-mimicking collagen-IV matrices trigger cellular EMT and invasion. Integr Biol (Camb) 2018;10:342-355. https://doi: 10.1039/c8ib00034d.
22. Wesseling M, Sakkers TR, de Jager SCA, Pasterkamp G, Goumans MJ. The morphological and molecular mechanisms of epithelial/endothelial-to-mesenchymal transition and its involvement in atherosclerosis. Vascul Pharmacol 2018;106:1-8. https://doi: 10.1016/j.vph.2018.02.006.
23. Mikami S, Oya M, Mizuno R, et al. Recent advances in renal cell carcinoma from a pathological point of view. Pathol Int 2016;66:481-490. https://doi: 10.1111/pin.12433.
24. Zeng J, Dou Y, Guo J, Wu X, Dai Y. Paeoniflorin of Paeonia lactiflora prevents renal interstitial fibrosis induced by unilateral ureteral obstruction in mice. Phytomedicine 2013;20:753-759. https://doi: 10.1016/j.phymed.2013.02.010.
25. Jang JW, Kim MK, Bae SC. Reciprocal regulation of YAP/TAZ by the Hippo pathway and the Small GTPase pathway. Small GTPases 2020;11:280-288. https://doi: 1080/21541248.2018.1435986.
26. Ni L, Luo X. Structural and biochemical analyses of the core components of the Hippo pathway. Methods Mol Biol 2019;1893:239-256. https://doi: 1007/978-1-4939-8910-2-18.

27. Kemppainen K, Wentus N, Lassila T, Laiho A, Törnquist K. Sphingosylphosphorylcholine regulates the Hippo signaling pathway in a dual manner. Cell Signal 2016;28:1894-1903. https://doi: 10.1016/j.cellsig.2016.09.004.

Tables

Table. 1, Overexpression of SIPA1L3 correlated with malignant phenotype in NSCLC patients

Clinicopathological Feature	N (217)	Overexpression (147)	$\chi 2$	*p*-value
Age(years)				
<57	95	62 (65.26%)	0.475	0.491
≥57	122	85 (69.67%)		
Gender				
Male	114	79 (69.30%)	0.266	0.606
Female	103	68 (66.02%)		
Histological Type				
squamous-cell carcinoma	83	53 (63.86%)	0.929	0.335
adenocarcinoma	134	94 (70.15%)		
Differentiation				
Well	117	71 (60.68%)	5.788	0.016
Moderate & Poor	100	76 (76.00%)		
Tumor status				
T1	124	74 (59.68%)	8.611	0.003
T2, T3, T4	93	73 (78.49%)		
TNM classification				
I+II	141	87 (61.70%)	6.721	0.010
III	76	60 (78.95%)		
Lymph node metastasis				
Positive	92	72 (81.52%)	8.087	0.004
Negative	125	75 (57.60%)		

TNM: tumor node metastasis

Figures

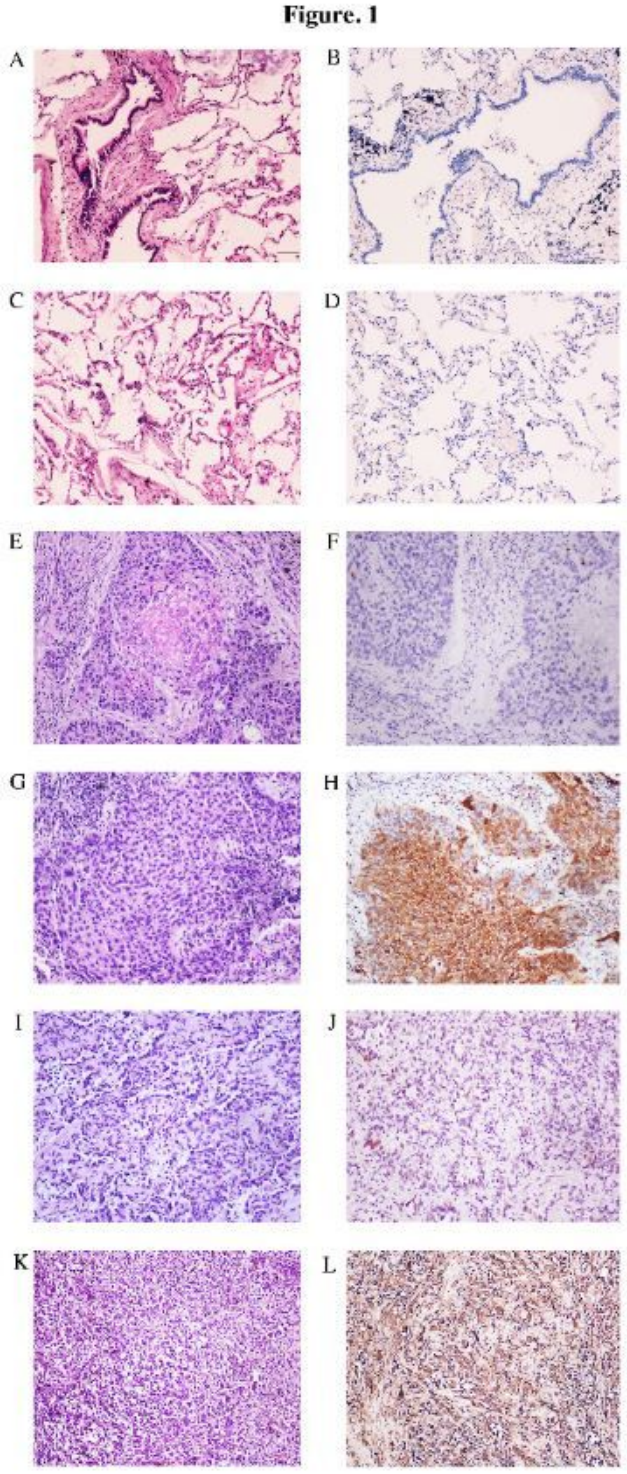

Figure 1

Immunohistochemistry analysis of SIPA1L3 expression in non–small cell lung cancer tissues. In normal bronchial epithelium (A) and alveolar epithelium (C), negative SIPA1L3 staining was detected by immunohistochemistry analysis (B, D). Well differentiated lung squamous cell carcinoma (E) showed negative SIPA1L3 staining (F). While cytoplasmic accumulation of SIPA1L3 protein was observed (H) in moderate & poor differentiation (G). Well differentiated adenocarcinoma (I) also showed the lower expression of SIPA1L3 (J) than that in poor differentiated adenocarcinoma (K, L). Bar, 100 μm.

Figure. 2

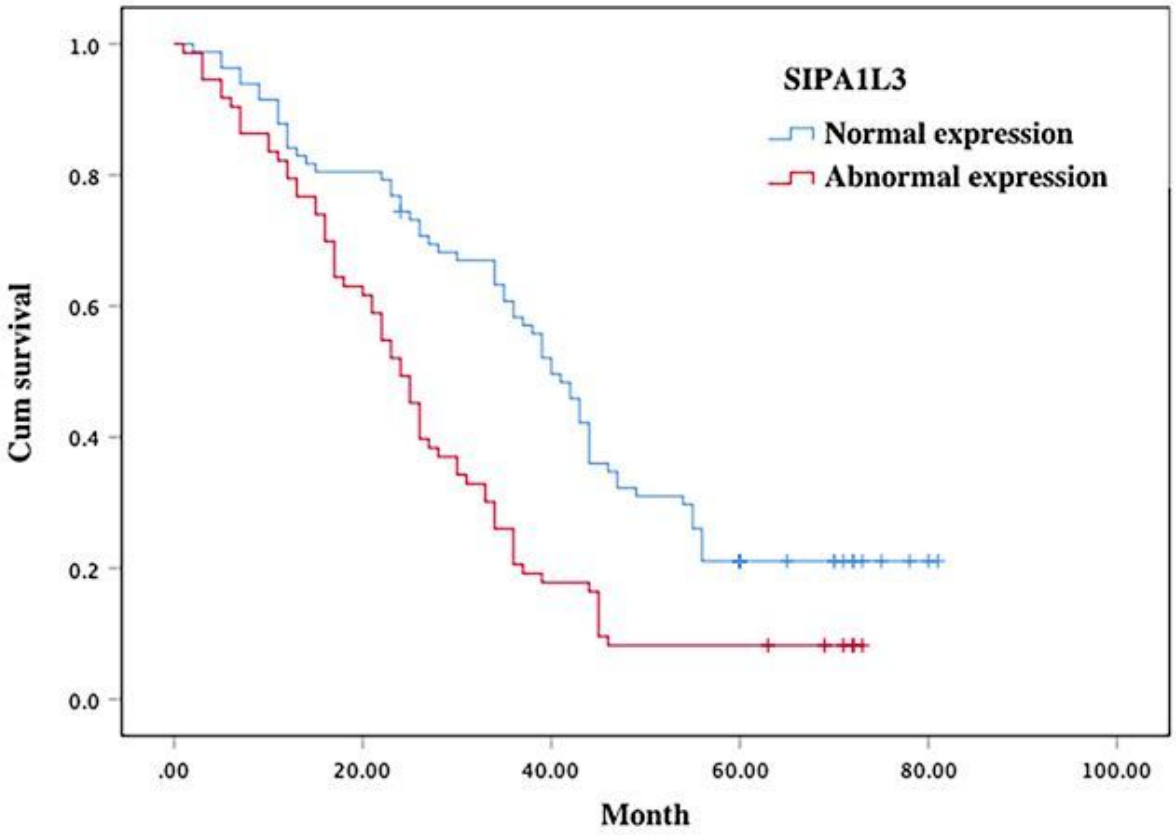

Figure 2

Overexpression of SIPA1L3 correlates with patient poor survival. Kaplan-Meier curves for the analysis of 155 patients with squamous cell carcinoma or adenocarcinoma stratified by SIPA1L3 expression. Patients with moderate to strong SIPA1L3 expression had a shorter survival time than patients with normal SIPA1L3 expression ($P < 0.001$).

Figure. 3

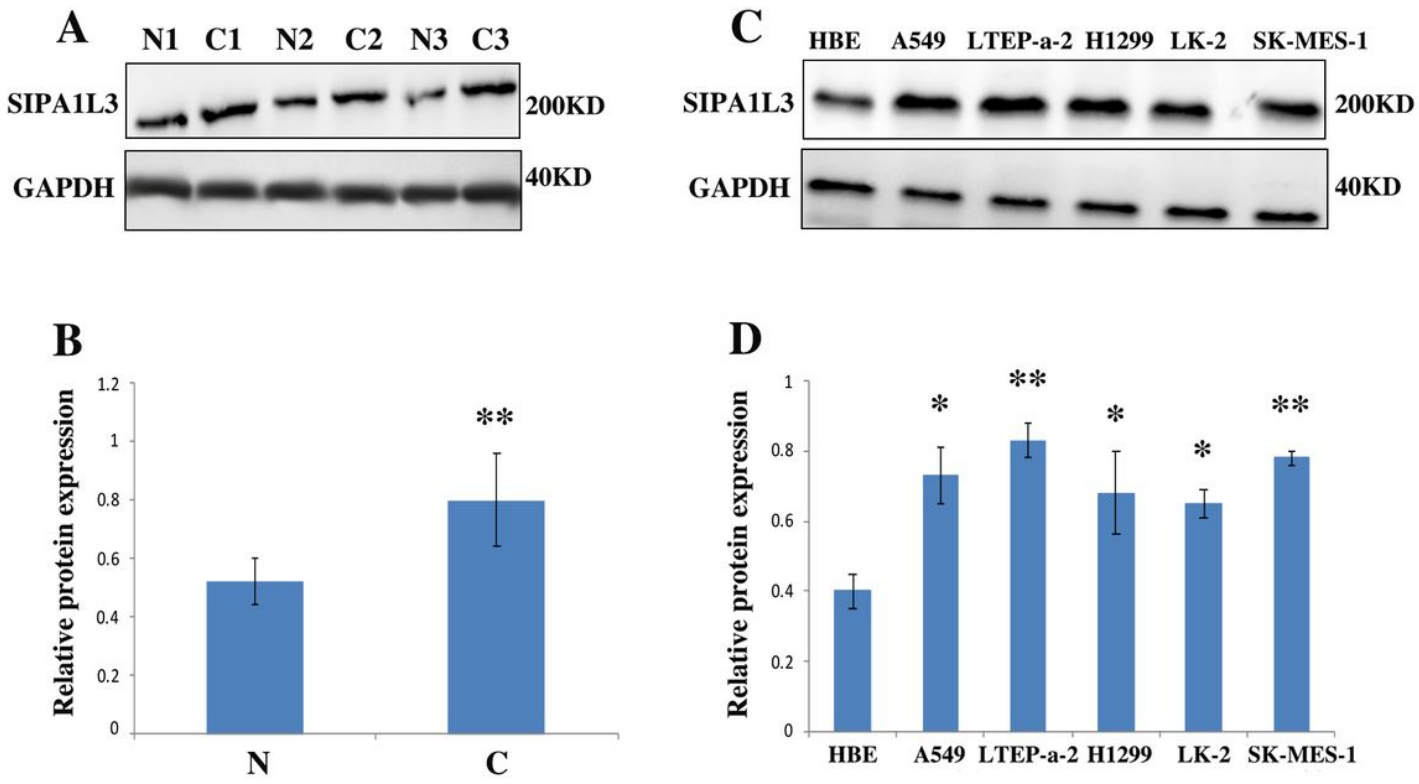

Figure 3

Western blot analysis of SIPA1L3 expression in lung cancer. (A) The bands of SIPA1L3 in lung adenocarcinoma samples (C1-C2) and SCC samples (C3-C4) had a higher signal intensity compared with matched normal lung tissues (N1-N4). (B) Increased SIPA1L3 expression was detected in different lung cancer cells compared to the immortalized bronchial epithelial cell line, HBE. Positions of the molecular weight markers are indicated. SIPA1L3 protein levels were normalized to GAPDH. Statistical analysis showed increased SIPA1L3 expression in lung cancer tissues (C; $P = 0.013$, N=40) and cell lines (D, $n \geq 3$; A549, $P = 0.029$; LTEP-a-2, $P = 0.011$; H1299, $P = 0.032$; LK-2, $P = 0.035$; and SK-MES-1, $P = 0.014$) compared to matched normal lung tissues.

Figure. 4

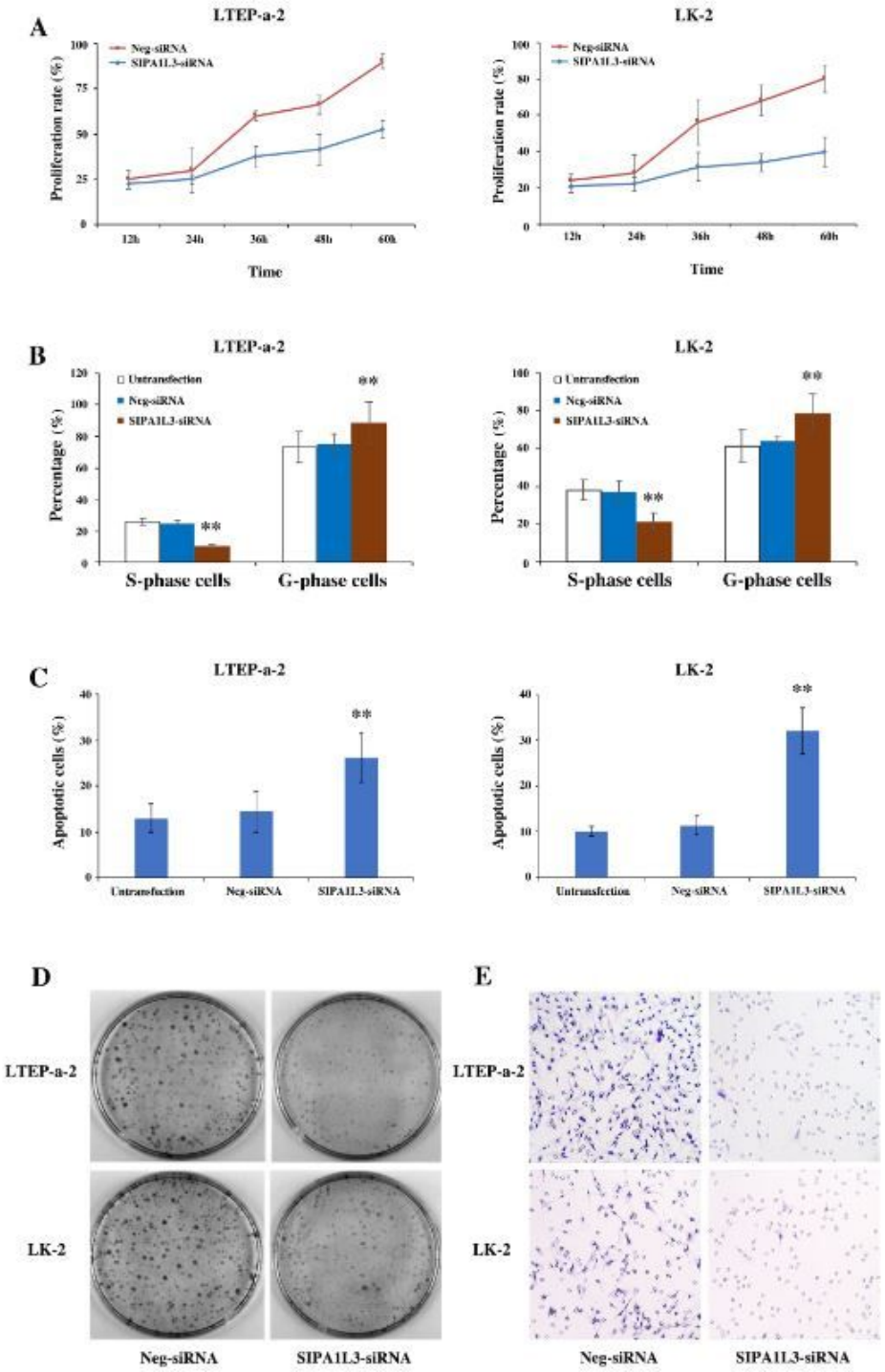

Figure 4

SIPA1L3 knockdown inhibited lung cancer cell growth and invasion. (A), MTT assay of LTEP-a-2 and LK-2 cells transfected with the SIPA1L3-siRNA plasmid. Both the LTEP-a-2 and LK-2 cell lines showed a time-dependent decrease in their cell proliferation rate after SIPA1L3-siRNA transfection, compared with the control groups. (B), Flow cytometry results for the cell cycle. Treatment with SIPA1L3-siRNA lead to a significant increase in the proportion of G-phase cells and a significant reduction in S-phase cells,

compared with untransfected and control cells. (C), Apoptotic cell death was determined by flow-cytometric analysis with Annexin V and PI staining. The percentage of apoptosis, including early and late stage of apoptotic cell death in each group. The result showed that knockdown of SIPA1L3 led to an increase of apoptotic cells compared with untransfected or control cells. (D), A significant decrease in colony numbers was observed in the LTEP-a-2 and LK-2 cells with downregulated SIPA1L3 compared with the controls. Colony numbers were counted under a microscope. ($P = 0.025$, $n \geq 3$; LTEP-a-2, Neg-siRNA vs. SIPA1L3-siRNA: 623 ±22 vs. 363 ± 14; LK-2, Neg-siRNA vs. SIPA1L3-siRNA: 510 ±22 vs. 214 ± 10). (E), The transwell assay showed that invading ability was significantly inhibited after SIPA1L3-siRNA transfection compared with the controls. ($P = 0.013$, $n \geq 3$, LTEP-a-2, Neg-siRNA vs. SIPA1L3-siRNA:305 ± 18 vs. 110 ± 12; LK-2, Neg-siRNA vs. SIPA1L3-siRNA:156 ± 11 vs. 43 ± 6)

Figure. 5

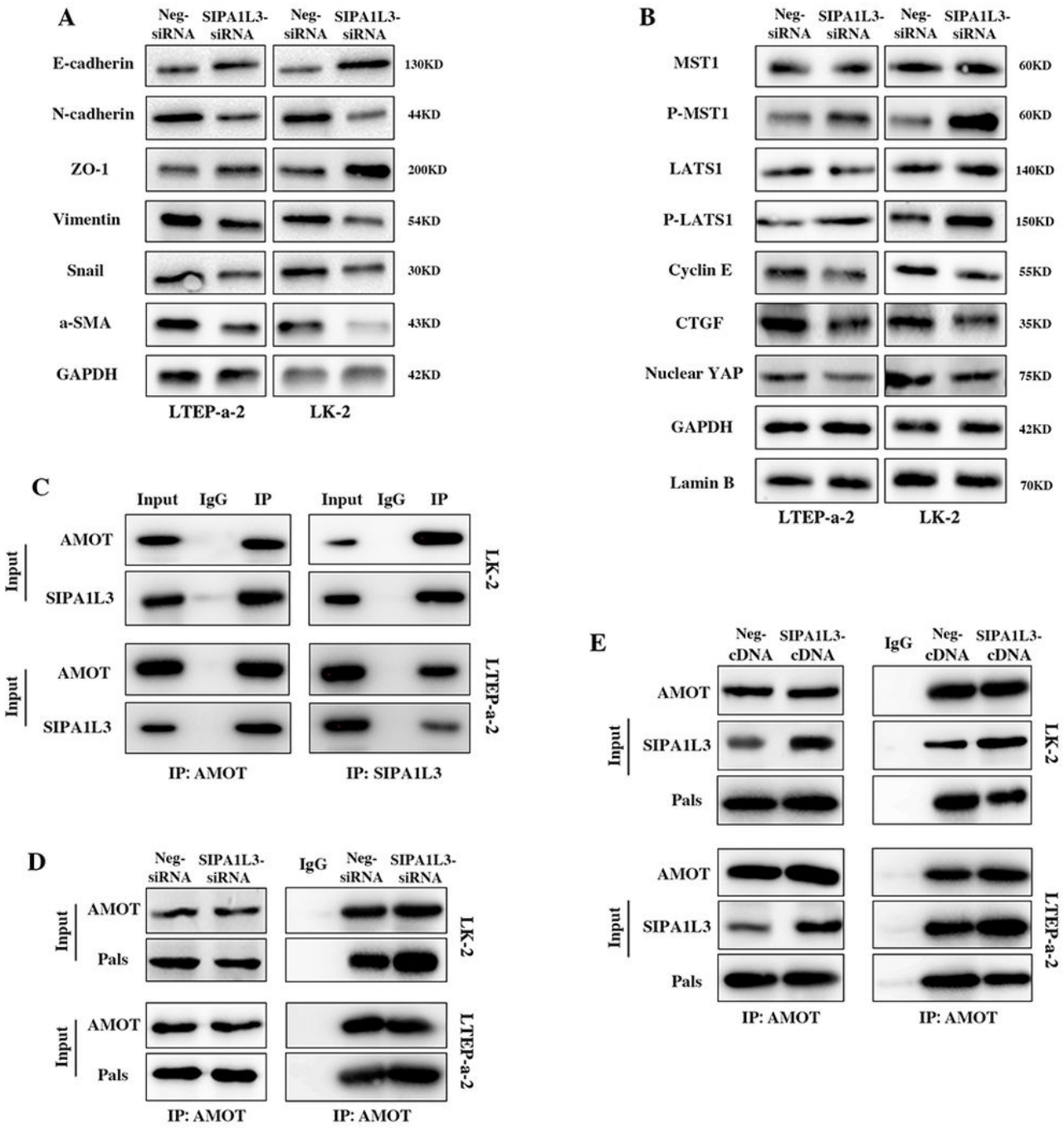

Figure 5

Downregulation of SIPA1L3 inhibited epithelial to mesenchymal transition (EMT) and activated the Hippo signaling pathway. (A), The main components of EMT, including E-cadherin, N-cadherin, ZO-1, Vimentin, Snail, and a-SMA, were measured by western blot in the lung cancer cell lines LTEP-a-2 and LK-2. In the cell lines with SIPA1L3-siRNA, the expression of E-cadherin and ZO-1 was significantly up-regulated, while the expression of N-cadherin, Vimentin, snail and a-SMA was significantly down-regulated. By western

blot, protein contents of MST1, p-MST1, LATS1, p-LATS1, nuclear YAP, Cyclin E, and CTGF were measured (B). Compared to those in the control LTEP-a-2 and LK-2 cells, SIPA1L3 knockdown increased p-MST1 and p-LATS1, while decreased the Cyclin E, CTGF, and nuclear YAP. (C), Immunocoprecipitation results showed the interaction between AMOT and SIPA1L3. (D), Immunocoprecipitation (quantitative) analysis showed increased binding of AMOT and Pals in SIPA1L3 knockdown cell lines. (E), Immunoprecipitation (quantitative) results showed that AMOT binding to SIPA1L3 increased and AMOT binding to Pals decreased in the cells transfection with SIPA1L3 compared to the control cells.

Supplementary Files

This is a list of supplementary files associated with this preprint. Click to download.

- SupplementaryFig.1.tif
- SupplementaryFig.2.tif